J. Fluid Mech. (1999), *vol.* 391, *pp.* 359–372. Printed in the United Kingdom

A generalization of Yaglom's equation which accounts for the large-scale forcing in heated decaying turbulence

By L. DANAILA[1], F. ANSELMET[1], T. ZHOU[2] AND R. A. ANTONIA[2]

[1]IRPHE, 12 Avenue Général Leclerc, 13003 Marseille, France
[2]Department of Mechanical Engineering, University of Newcastle, NSW, 2308, Australia

(Received 11 August 1998 and in revised form 24 March 1999)

In most real or numerically simulated turbulent flows, the energy dissipated at small scales is equal to that injected at very large scales, which are anisotropic. Despite this injection-scale anisotropy, one generally expects the inertial-range scales to be locally isotropic. For moderate Reynolds numbers, the isotropic relations between second-order and third-order moments for temperature (Yaglom's equation) or velocity increments (Kolmogorov's equation) are not respected, reflecting a non-negligible correlation between the scales responsible for the injection, the transfer and the dissipation of energy. In order to shed some light on the influence of the large scales on inertial-range properties, a generalization of Yaglom's equation is deduced and tested, in heated grid turbulence ($R_\lambda = 66$). In this case, the main phenomenon responsible for the non-universal inertial-range behaviour is the non-stationarity of the second-order moments, acting as a negative production term.

1. Introduction

The traditional concept of the energy cascade in turbulent flows offers a simple scenario for the transfer from large injection scales down to small dissipative scales. In fact, the energy injection in the large scales is a necessary 'source' for the transfer and dissipation through all the scales. The way energy is injected is specific to each flow and mixing configuration, and is arguably not important to a certain range of scales, referred to as the inertial range (IR). Therefore, one expects the IR to be locally isotropic, at least at very large Reynolds numbers, as explained in Monin & Yaglom (1975). These considerations are central to the well-known Kolmogorov theory (K41). Similar considerations apply to a passive scalar field, as it was argued in Oboukhov (1949) and Corrsin (1951). In the context of isotropy, a relatively simple relation was obtained by Yaglom (Yaglom 1949), see also Monin & Yaglom (1975), between the second-order moment of the temperature increment $\Delta\theta = \theta(x_1 + r) - \theta(x_1)$ and the third-order mixed moment $\langle \Delta u_1 (\Delta\theta)^2 \rangle$ (the angular brackets denote time averaging), where Δu_1 is the longitudinal velocity increment. Yaglom's equation is

$$\tfrac{4}{3}\langle \epsilon_\theta \rangle r = -\langle \Delta u_1 (\Delta\theta)^2 \rangle + 2k \frac{\mathrm{d}}{\mathrm{d}r} \langle (\Delta\theta)^2 \rangle, \tag{1.1}$$

where $\langle \epsilon_\theta \rangle = k \left(\langle \theta_1^2 \rangle + \langle \theta_2^2 \rangle + \langle \theta_3^2 \rangle \right)$ is the mean temperature dissipation rate, k is the molecular diffusivity, and $\theta_{,i} = \partial\theta/\partial x_i$ is the spatial derivative of θ in the ith direction (x_1 is the streamwise direction). Equation (1.1) is of capital importance to turbulence research, being the only relation which is directly deduced from the heat transport equation. Reasonably good agreement with (1.1) is generally obtained (e.g. Monin & Yaglom 1975 and Antonia, Chambers & Browne 1983) for small and intermediate scales, the level of agreement for the IR scales being obviously improved when the Reynolds number increases.

Thus, local isotropy and (1.1) should be satisfied in the IR of any flow, irrespectively of the large-scale properties or the energy injection mode. A distinction can however be made between continuous injection and decaying flows.

(*a*) *Continuous-injection flows.* This class includes flows where the injection occurs through large-scale velocity and temperature gradients. Typical examples are the slightly heated boundary layer, the swirling flow between two heated (or cooled) disks, and the direct numerical simulations (DNS) of an isotropic velocity field where the temperature dissipation rate is fed by a large-scale mean-temperature gradient. The property common to this flow category is the presence of a large-scale mean temperature gradient: $\boldsymbol{G}$. The term 'continuous' is supported by the fact that $\boldsymbol{G}$ is stationary in time, leading to the stationarity of all other statistical quantities. Experiments (Mestayer 1982; Sreenivasan 1991; Sreenivasan & Tavoularis 1980) and simulations (Holzer & Siggia 1994 and Pumir 1994*a*) have shown that the role of $\boldsymbol{G}$ is important down to the very small scales, resulting in a non-zero temperature-derivative skewness at least in the direction parallel to $\boldsymbol{G}$. This violates local isotropy.

(*b*) *Decaying flows.* The initial condition plays a major role. Subsequent to the energy injection, the flow decays until the energy is totally dissipated. This category includes

(i) Grid turbulence. This is the simplest flow, providing a close approximation to isotropy. Note that there have been studies of grid turbulence in combination with an initial condition for the passive scalar field such as a mean temperature gradient, as it was done in Budwig, Tavoularis & Corrsin (1985), Tong & Warhaft (1994) and Mydlarski & Warhaft (1998). This increases the complexity, even though it preserves the characteristics of a decaying flow entirely.

(ii) Jets and wakes. These are relatively more complex flows. Along the axis or plane of symmetry, there is both streamwise decay and a relatively strong radial or transverse turbulent diffusion.

Grid turbulence with quasi-isotropic initial conditions seems to be the simplest case of freely decaying flows. Isotropy of small scales is generally verified, although there may be exceptions, to be discussed later, associated with the injection mode. Strategies can be used to improve the isotropy of grid turbulence, either experimentally, as seen in Comte-Bellot & Corrsin (1966) or in Antonia *et al.* (1978), or numerically in Boratav & Pelz (1994).

While Sreenivasan (1996) has already distinguished between grid turbulence and turbulent shear flows in the context of the relative spectral scalings of velocity and temperature, a formal distinction has yet to be made. The aim of the present paper is to identify, both qualitatively and quantitatively, the origin of the non-balance between the different terms in (1.1), for relatively small Reynolds numbers, in decaying thermal grid turbulence. We will briefly describe the experimental set-up in § 2. The verification of the generalized form of Yaglom's equation, where the contribution from an additional large-scale injection term is included, is presented in § 3.

2. Experimental details

Measurements were made on the centreline of the working section (350 mm × 350 mm, 2.4 m long) of a non-return blower-type wind tunnel, downstream of a biplane grid, in the range $20 \leqslant x_1/M \leqslant 80$ (M is the mesh size of the grid). The mean longitudinal velocity of the flow, U_1, was 7 ms^{-1}. A square mesh ($M = 24.76$ mm, with 4.76 mm × 4.76 mm square rods) grid, with a solidity of 0.35, was used.

A mandoline was used to heat the flow in a way similar to Warhaft & Lumley (1978). For all the measurements, the mandoline was fixed at $1.5M$ downstream of the grid. It was constructed from fine Chromel-A wires of 0.5 mm diameter. The mandoline comprised two parts separated by 15 mm in the streamwise direction: the wires were horizontal in one and vertical in the other. Each part had a resistance of about 22 Ω and was heated by a power supply with a total power consumption of about 2 kW for both. The mean temperature ΔT relative to ambient was about 3 K in the tunnel. The wire separation in each part was 24.76 mm, i.e. the same as M. To prevent sagging due to thermal expansion, small springs were used to keep each wire under tension.

Simultaneous measurements of the three components of velocity and temperature were conducted, using a probe comprising 2 X-wires and a cold wire. One X-wire was in the (x_1, x_2)-plane, and the other one was in the (x_1, x_3)-plane. To avoid contamination of the cold wire measurements from the hot wires, the cold wire was located 1 mm below the centre of the two X-wires and shifted 0.5 mm upstream. The probe was calibrated at the centreline of the tunnel against a Pitot tube connected to a MKS baratron pressure transducer (the least count is 0.01 mm H_2O). The yaw calibration was performed over a range of $\pm 20^\circ$ in both the (x_1, x_2)- and (x_1, x_3)-planes.

The wires were etched from Wollaston Pt–10% Rh . The active length of the cold wire was about $800d_w$ ($d_w = 0.63$ μm is the wire diameter). For the hot wires, the diameter was $d_w = 2.5$ μm, the length of the active part being $200d_w$. The hot wires were operated with in-house constant-temperature anemometers with an overheat ratio of 1.5. The cold wire was operated with a constant-current (0.1 mA) circuit, also built in-house. The output signals from the constant-current and constant-temperature anemometers were passed through buck and gain circuits, and low-pass filtered at a cut-off frequency f_c close to f_K, the Kolmogorov frequency (estimated via $f_K = U_1/2\pi\eta$, where η is the Kolmogorov length scale). The cut-off frequency is therefore a function of the position behind the grid: it varies from 5 kHz at $x_1/M = 20$ to 1.6 kHz at $x_1/M = 80$. The signals were then digitized into a personal computer using a 12 bit A/D converter at a sampling frequency of $2f_c$. The record duration was 52 s. The data were analysed on a VAX 780 computer.

The instantaneous velocity signals were corrected for the influence of temperature fluctuations using the following relation:

$$E^2 \frac{T_w - T_1}{T_w - T} = A + BU^n,$$

where A, B and n are the calibration constants at ambient temperature, T_1; T_w is the hot-wire temperature, T is the instantaneous fluid temperature measured by the cold wire; E and U are the instantaneous voltage and longitudinal velocity ($\equiv U_1 + u_1$), respectively.

Velocity and temperature increments were computed using Taylor's hypothesis. This should be satisfactory since the local turbulence intensity u_1'/U_1 is less than 2% in the present experiment (the prime denotes the r.m.s. value).

The Taylor microscale Reynolds number, defined as $R_\lambda = \lambda_{u_1} u_1'/\nu \approx 66$, where $\lambda_{u_1}^2 = u_1'^2/\langle(\partial u_1/\partial x_1)^2\rangle$, is approximately constant in x_1. The components of the energy dissipation rate, measured in a separate experiment, satisfy isotropy very well (within $\pm 10\%$), after adequate corrections are applied (Antonia, Zhou & Zhu 1998). Local isotropy of the temperature field has been verified in this flow in a previous investigation (Danaila *et al.* 1999). The temperature field satisfies homogeneity quite closely. ΔT is constant to within 1% in all directions, whereas $\langle\theta^2\rangle$, the temperature variance, is uniform within 10% in the directions normal to the stream. The probability density functions of temperature and velocity increments are symmetrical about the ordinate, irrespectively of the scale. The p.d.f.s of the three temperature derivatives are nearly identical. Consistently, the skewness of the temperature derivative is almost zero (≈ 0.01), for $i = 1, 2$ and 3. This is evidence that the small-scale structure of the dynamic and passive scalar fields is nearly isotropic. Note here that in a continuous injection flow, the presence of $\boldsymbol{G}$ leads to a non-zero temperature-derivative skewness, independently of R_λ, as emphasized by Sreenivasan (1991) or Pumir (1994*b*).

In grid turbulence, isotropy and homogeneity are usually well verified in a plane normal to the stream. Such good agreement is not expected in the streamwise direction, reflecting the role of the non-stationarity. The decay of different quantities such as velocity and temperature variances $\langle u_1^2\rangle$, $\langle u_2^2\rangle$, $\langle u_3^2\rangle$, $\langle\theta^2\rangle$ is characterized by a power-law of the type

$$\langle u_1^2\rangle \approx \left(\frac{x_1}{M}\right)^{-m_{u1}}.$$

Magnitudes of m_{u1}, m_{u2}, m_{u3} and m_θ have been previously reported by Comte-Bellot & Corrsin (1966) and Warhaft & Lumley (1978). They provide a basis of comparison between the passive scalar behaviour and that of any of the velocity components. In the present flow, $m_\theta \approx 1.42$ is much closer to $m_{u2} \approx m_{u3} \approx 1.39$, than to $m_{u1} \approx 1.3$, indicating that the decay of θ is similar to that of u_2 or u_3. The decay of the temperature fluctuating field does not depend on the temperature ΔT, but it seems to depend strongly on the injection mode: the grid (and mandoline) mesh M and the distance between the grid and the mandoline, as investigated by Sreenivasan *et al.* (1980) or Durbin (1982). Also, the decay of the temperature variance can be simplified to

$$U_1 \frac{\mathrm{d}}{\mathrm{d}x_1}\langle\theta^2\rangle/2 = -\langle\epsilon_\theta\rangle, \tag{2.1}$$

which has already been verified within $\pm 10\%$ (Danaila *et al.* 1999). This equation is obtained using the local homogeneity assumption, only. Local isotropy is not required here. In the following discussion, this relation is important for the development of our generalized Yaglom's equation. The results presented hereafter are obtained using the approximation $\langle\epsilon_\theta\rangle = \langle\epsilon_\theta\rangle_{iso} = 3k\langle(\partial\theta/\partial x_1)^2\rangle$.

The conclusion here is that the small-scale passive scalar field in grid turbulence verifies isotropy and symmetry quite satisfactorily. Note however that other quantities, such as the correlation coefficients between the increments of temperature and any of the velocity components, are not zero, as they should be if isotropy were strictly verified. The non-zero values of these quantities reflect the initial coupling between velocity and temperature fields.

3. Generalized form of Yaglom's equation

In this Section, we will analyse in great detail Yaglom's equation (1.1). In what follows, we use the dimensionless separation r^*, where the superscript $*$ denotes

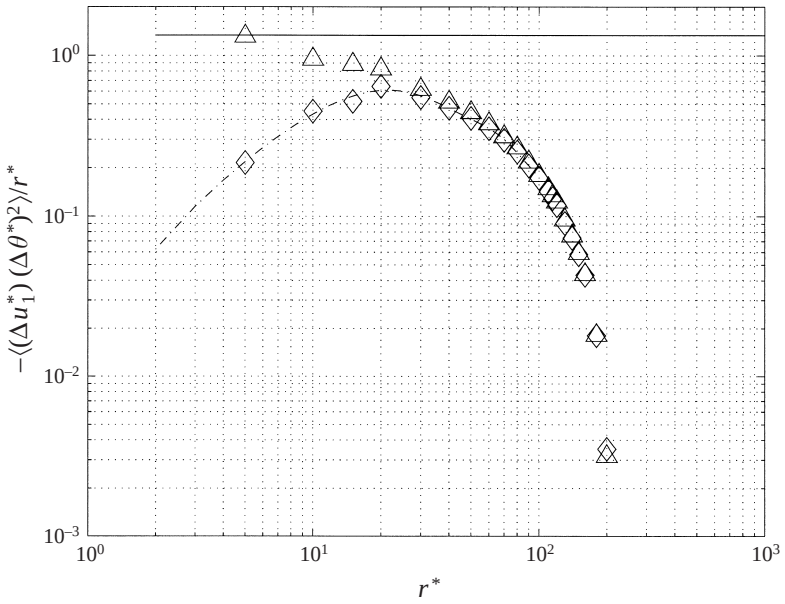

FIGURE 1. Comparison between the two terms in (3.1), at $x_1/M = 70$: $\diamond$, A (computed using measurements), the dotted line is a polynomial least-squares fit. The solid horizontal line represents $\frac{4}{3}$. $\triangle$, The sum of the turbulent transport term and the dissipative term in (1.1).

normalization by the Kolmogorov length scale, $\eta = \left(\nu^3/\langle\epsilon\rangle\right)^{1/4}$ (where ν is the kinematic viscosity of air and $\langle\epsilon\rangle$ is the mean turbulent energy dissipation rate which was determined in a separate experiment with the same experimental conditions, using both isotropy and the decay rate of the mean turbulent kinetic energy), the Kolmogorov velocity scale $u_K = \left(\nu\langle\epsilon\rangle\right)^{1/4}$ or the temperature scale $\theta_K = (\langle\epsilon_\theta\rangle\eta/u_K)^{1/2}$. The magnitude of η depends on x_1, varying from 0.22 mm at $x_1/M = 20$ to 0.50 mm at $x_1/M = 80$.

In the IR, (1.1) reduces, in non-dimensional form, to

$$\tfrac{4}{3} = -\langle(\Delta u_1^*)(\Delta\theta^*)^2\rangle/r^*. \tag{3.1}$$

Figure 1 shows the balance between the right-hand side of (3.1), denoted for simplicity by A, and the constant $\frac{4}{3}$. At this relatively small Reynolds number, the balance is clearly not satisfied. The turbulent transport does not attain the level corresponding to that for total dissipation, presumably because the correlation between large and small scales is not negligible. In contrast, the total contribution from A and the dissipative term in (1.1), denoted by B, seems to reach $\frac{4}{3}$, but only for $r^* \leqslant 5$. This is required as a consequence of the definition of $\langle\epsilon_\theta\rangle$ and our observation that small-scale isotropy is satisfied for second-order moments, as explained in Antonia *et al.* (1983).

Note here that the effect of the small Reynolds number on the second-order moments (or spectra) has already been investigated for different flows, by Sreenivasan (1996). On the other hand, the Reynolds number effect was also investigated for the third-order moments, in active grid turbulence by Mydlarski & Warhaft (1998) and in numerical simulations of turbulent flows by Yeung & Zhou (1997). The constant $\frac{4}{3}$ (or its velocity counterpart $\frac{4}{5}$) is apparently only obtained at a minimum value of R_λ of about 400 (Mydlarski & Warhaft 1998).

To our knowledge, there has been no previous study aimed at understanding the physical significance of the difference between the two terms of (3.1). To this end, we carefully reconsider the derivation of (1.1), as presented in Monin & Yaglom (1975). We start with the heat transport equation, at $\boldsymbol{x}$:

$$\frac{\partial \theta}{\partial t} + \boldsymbol{u} \cdot \nabla \theta = k \nabla^2 \theta, \tag{3.2}$$

where $\boldsymbol{u} = (u_1, u_2, u_3)$ is the fluctuating velocity field. Since the aim is to investigate the behaviour of the mixed velocity–temperature moments, using an increment $\boldsymbol{r}$, we now write the same equation at $\boldsymbol{x} + \boldsymbol{r}$. All the quantities at this location are designated by the superscript $+$:

$$\frac{\partial \theta^+}{\partial t} + \boldsymbol{u}^+ \cdot \nabla^+ \theta^+ = k \nabla^{2+} \theta^+. \tag{3.3}$$

After multiplying (3.2) by θ^+, adding it to relation (3.3) multiplied by θ, and averaging, we obtain

$$\frac{\partial}{\partial t} \langle \theta \theta^+ \rangle - 2 \nabla_{\boldsymbol{r}} \langle \boldsymbol{u} \theta \theta^+ \rangle = 2k \nabla_{\boldsymbol{r}}^2 \langle \theta \theta^+ \rangle. \tag{3.4}$$

Equation (3.4) was in fact originally derived by Corrsin (1951). With the further use of local homogeneity and isotropy, the gradient and Laplacian operators involved in (3.4) can be expressed using only the modulus r of $\boldsymbol{r}$:

$$\nabla_{\boldsymbol{r}} = \frac{2}{r} + \frac{\partial}{\partial r}, \quad \nabla_{\boldsymbol{r}}^2 = \left[\frac{2}{r} + \frac{\partial}{\partial r} \right] \frac{\partial}{\partial r}. \tag{3.5}$$

Substituting (3.5) into (3.4),

$$\frac{\partial}{\partial t} \langle \theta \theta^+ \rangle = 2 \left[\frac{2}{r} + \frac{\partial}{\partial r} \right] \left[\langle u_1 \theta \theta^+ \rangle + k \frac{\partial}{\partial r} \langle \theta \theta^+ \rangle \right]. \tag{3.6}$$

Using local homogeneity and isotropy,

$$\left.\begin{aligned} \langle \theta \theta^+ \rangle &= \langle \theta^2 \rangle - \tfrac{1}{2} \langle (\Delta \theta)^2 \rangle, \\ \langle u_1 \theta \theta^+ \rangle &= \tfrac{1}{4} \langle \Delta u_1 (\Delta \theta)^2 \rangle. \end{aligned}\right\} \tag{3.7}$$

Substituting (3.7) into (3.6), where the previously verified relation (2.1) was used, multiplying by r^2, integrating with respect to r and dividing by r^2, we finally obtain

$$-\tfrac{4}{3} \langle \epsilon_\theta \rangle r - \frac{1}{r^2} \int_0^r y^2 \frac{\partial}{\partial t} \langle (\Delta \theta)^2 \rangle \mathrm{d}y = \langle \Delta u_1 (\Delta \theta)^2 \rangle - 2k \frac{\mathrm{d}}{\mathrm{d}r} \langle (\Delta \theta)^2 \rangle, \tag{3.8}$$

where y is a 'dummy' variable here identifiable with the separation. The temperature second-order moments used in the integral are computed using a separation y, the modulus of the vector $\boldsymbol{y}$, i.e.

$$\langle (\Delta \theta)^2 \rangle = \langle (\theta(\boldsymbol{x} + \boldsymbol{y}) - \theta(\boldsymbol{x}))^2 \rangle.$$

For simplicity, we keep the same notation for the temperature second-order moments.

By comparison to (1.1), equation (3.8) has one additional term:

$$S = -\frac{1}{r^2} \int_0^r y^2 \frac{\partial}{\partial t} \langle (\Delta \theta)^2 \rangle \mathrm{d}y, \tag{3.9}$$

which results simply from the presence of the second-order moment in relation (3.7). The operators which act on the temperature second-order moments in order to obtain (3.9) are the same as those which are applied to (3.6) for obtaining (3.8).

The supplementary term S reflects the influence of the time derivative of $\langle(\Delta\theta)^2\rangle$. This derivative can be evaluated using Taylor's hypothesis, since $\langle(\Delta\theta)^2\rangle$ was measured at several positions downstream of the grid. Specifically, S is evaluated from the relation

$$S = -\frac{U_1}{r^2}\int_0^r y^2 \frac{\partial}{\partial x_1}\langle(\Delta\theta)^2\rangle \mathrm{d}y.$$

We comment here on a subtle aspect of grid turbulence, regarding homogeneity. This flow is not globally homogeneous because, along the mean flow direction, some quantities, such as $\langle\theta^2\rangle$, are not constant. The characteristic scale of this decay has a magnitude of about $10M$, much larger than the characteristic scale of the mixing (for instance, the injection scale is about $M/2 \approx 60\eta$). This significant difference allows us to characterize the mixing in grid turbulence as

locally homogeneous at the characteristic scales of the mixing, where the operators ∇_r and ∇_r^2 act – the term 'local' homogeneity (or isotropy), already used in Monin & Yaglom (1975) and rediscussed by Hill (1997), means that this concept is valid over a limited range of scales, those which are much smaller than the large injection scales;

globally non-homogeneous at large scales ($\approx 10M$), where the decay dominates.

The physical picture that we can ascribe to these two notions is that of a sphere of radius r (the considered scale) much smaller than the scales that this sphere explores. The physical properties of the mixing in this sphere are (locally) homogeneous and isotropic; such scales, which could be thought of as 'rapid', are characterized by local homogeneity and isotropy. On the other hand, the large scales, which may be viewed as 'slow', are characterized by a global non-homogeneity.

The fundamental difference between grid turbulence and other (shear) flows is the fact that all even moments of temperature, as well as velocity, are not stationary in decaying flows, but evolve continuously in the streamwise direction x_1. In continuous-injection flows (group (*a*), § 1), all the moments are nearly stationary so that their time, or x_1 evolution, can be neglected, as in Yaglom's equation (1.1).

We emphasize here that, for the simplest flow in group (*b*), it is necessary to take into account the decay of $\langle(\Delta\theta)^2\rangle$ in order to close the relations correctly. Note also that, for group (*a*), the generalization of Yaglom's equation could be carried out, though using a different approach. The starting point remains the heat transport equation, but with a 'source term' $\boldsymbol{Gu}$, as explained in Pumir (1994*a*), and proper account taken of the stationarity of all moments and of the particular flow geometry. An appropriate form of equation (2.1) could be deduced by replacing the time decay of the temperature variance by diffusion along the anisotropic direction, i.e. the mean temperature gradient direction. The generalized form of Yaglom's equation would then take explicitly into account the presence of the mean temperature gradient. Therefore, it is not possible to write a 'unified' form for the supplementary terms in Yaglom's equation for different flow categories (groups (*a*) and (*b*)). The significance of these terms depends on the nature of the large scales injecting the energy, which will obviously differ for the different flow categories.

We now turn our attention to (3.8), written for simplicity as

$$\tfrac{4}{3}r^* = A + B + S^*, \tag{3.10}$$

where A is the turbulent transport term ($A = -\langle\Delta u(\Delta\theta)^2\rangle/(u_K\theta_K^2)$), B is the small-scale diffusion term ($B = 2k(\mathrm{d}/\mathrm{d}r^*)\langle(\Delta\theta)^2\rangle/(\langle\epsilon_\theta\rangle\eta^2)$), and S^* represents the additional

source term, in its dimensionless form. The term S^* is estimated as

$$S^* = -\frac{U_1}{\langle \epsilon_\theta \rangle} \frac{1}{r^{*2}} \int_0^{r^*} y^{*2} \frac{\partial}{\partial x_1} \langle (\Delta\theta)^2 \rangle \mathrm{d}y^*.$$

Now, in order to obtain the value of $(\partial/\partial x_1)\langle(\Delta\theta)^2\rangle$, we need an additional assumption, that the temperature second-order moments are 'self–similar' for different positions behind the grid. Mathematically, we decompose

$$\langle (\Delta\theta)^2 \rangle (r, x_1) \equiv f(r)\, g(x_1),$$

where $f(r)$ is the 'shape' function, and $g(x_1)$ is the 'decaying' part of the second-order moments. This assumption has some experimental support, given that the turbulent Reynolds number R_λ is approximately constant with respect to x_1. Specifically, the two functions are

$$f(r) \equiv \langle (\Delta\theta)^2 \rangle / \langle \theta^2 \rangle = \text{constant};$$

$$g(x_1) \equiv \langle \theta^2 \rangle.$$

Next, we evaluate

$$\frac{\partial}{\partial x_1} \langle (\Delta\theta)^2 \rangle = \frac{\langle (\Delta\theta)^2 \rangle}{\langle \theta^2 \rangle} \frac{\partial}{\partial x_1} \langle \theta^2 \rangle,$$

and, since the variables x_1 and y (which represents a separation) are independent, we write

$$S^* = -\frac{1}{\langle \epsilon_\theta \rangle} \left[U_1 \frac{\partial}{\partial x_1} \langle \theta^2 \rangle \right] \frac{1}{r^{*2}} \int_0^{r^*} y^{*2} \frac{\langle (\Delta\theta)^2 \rangle}{\langle \theta^2 \rangle} \mathrm{d}y^*.$$

Using relation (2.1),

$$S^* = 2 \frac{1}{r^{*2}} \int_0^{r^*} y^{*2} \frac{\langle (\Delta\theta)^2 \rangle}{\langle \theta^2 \rangle} \mathrm{d}y^*,$$

so that differentiation of $\langle \theta^2 \rangle$ with respect to x_1 is avoided, thus improving the estimation of S^*. The uncertainty of this latter quantity essentially reflects the uncertainty in verifying (2.1).

All the terms in (3.10) are shown in figure 2. As previously noted, Yaglom's equation, which expresses the balance $A + B = \frac{4}{3} r^*$, is verified for scales smaller than 5η. The additional source term S^* inherits somewhat the behaviour of $\langle (\Delta\theta)^2 \rangle$ which features in the integrand of (3.9). The balance between $\frac{4}{3} r^*$ and $A+B+S^*$ is quite good for $r^* \leqslant 200$, underlining the fact that the decay is crucial in this type of flow. In a different context, it validates, to a good approximation, the three-dimensional isotropy of the passive scalar field in grid turbulence. The behaviour of A for $r^* \geqslant 200$ suggests that the record duration may be insufficient for the convergence of the mixed-order moments.

The following remarks can also be made in connection with the large-scale agreement of (3.10). For scales larger than about 200η, the spatial correlations vanish, so that some of the quantities are stationary in r^*. A is approximately zero, whereas the temperature second-order moment has a constant value,

$$\langle (\Delta\theta)^2 \rangle = 2 \langle \theta^2 \rangle.$$

An immediate consequence of these observations is that, for $r^* \gg 200$, or $r^* \to \infty$,

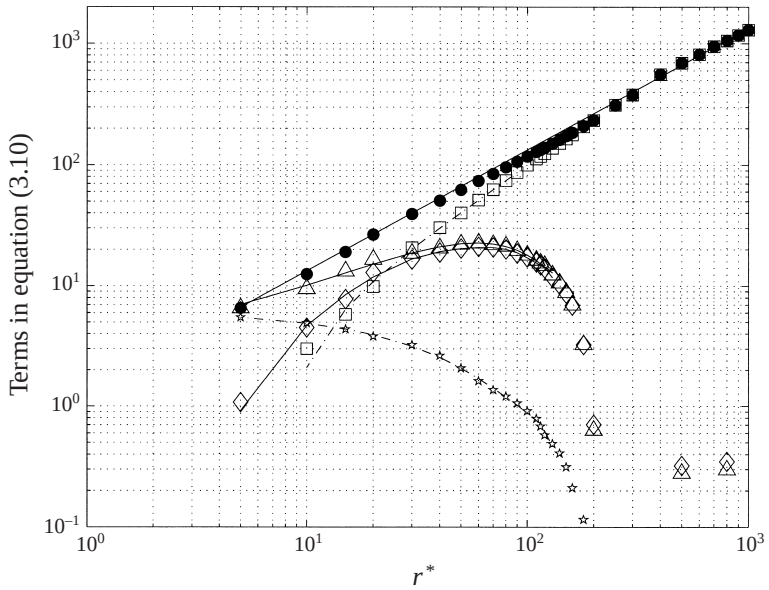

FIGURE 2. Verification of (3.10) at $x_1/M = 70$: $\diamond$, the turbulent transport A (the continuous line is a polynomial interpolation of these values); $\star$, the small-scale diffusion term B (the dotted line is a polynomial interpolation), the straight line is $\frac{4}{3}r^*$; $\square$, the source term S^*; $\triangle$, $A+B$; $\bullet$, $A+B+S^*$.

(3.10) reduces to

$$\begin{aligned}\tfrac{4}{3}r^* = S^* &= -\frac{1}{\langle\epsilon_\theta\rangle}\frac{U_1}{r^{*2}}\lim_{r^*\to\infty}\int_0^{r^*} y^2\frac{\partial}{\partial x_1}\langle(\Delta\theta)^2\rangle \mathrm{d}y \\ &= -\frac{1}{\langle\epsilon_\theta\rangle}\frac{U_1}{r^{*2}}\int_0^{200} y^2\frac{\partial}{\partial x_1}\langle(\Delta\theta)^2\rangle \mathrm{d}y - \frac{1}{\langle\epsilon_\theta\rangle}\frac{U_1}{r^{*2}}\int_{200}^{r^*} y^2\frac{\partial}{\partial x_1}\langle(\Delta\theta)^2\rangle \mathrm{d}y \\ &\approx -\frac{1}{\langle\epsilon_\theta\rangle}\frac{U_1}{r^{*2}}\int_{200}^{r^*} y^2\frac{\partial}{\partial x_1}\langle(\Delta\theta)^2\rangle \mathrm{d}y.\end{aligned}$$

Since, for $r^* \geqslant 200$, $\langle(\Delta\theta)^2\rangle \approx 2\langle\theta^2\rangle$, we finally have

$$\tfrac{4}{3}r^* = S^* \approx -\frac{2}{\langle\epsilon_\theta\rangle}\frac{U_1}{r^{*2}}\int_0^{r^*} y^2\frac{\partial}{\partial x_1}\langle\theta^2\rangle \mathrm{d}y. \tag{3.11}$$

Since $\langle\theta^2\rangle$ does not depend on r^*, and x_1 and r^* are independent variables, we obtain

$$\tfrac{4}{3}r^* = -\frac{2r^*}{3\langle\epsilon_\theta\rangle}U_1\frac{\partial\langle\theta^2\rangle}{\partial x_1}, \tag{3.12}$$

which is identical with (2.1). This calculation highlights the link between the large-scale verification of (3.10) and (2.1), the slight disagreement observed in figure 2 for the large scales reflecting the uncertainty ($\pm 10\%$) in verifying (2.1). It should be emphasized that grid turbulence, which allows such a simple verification of the equation for $\langle\epsilon_\theta\rangle$, is the only flow which permits Yaglom's equation to be generalized in such a simple manner.

Note here that the large-scale agreement we obtain with (3.10) is essentially linked to the validity of (2.1) in grid turbulence, for which only local homogeneity is

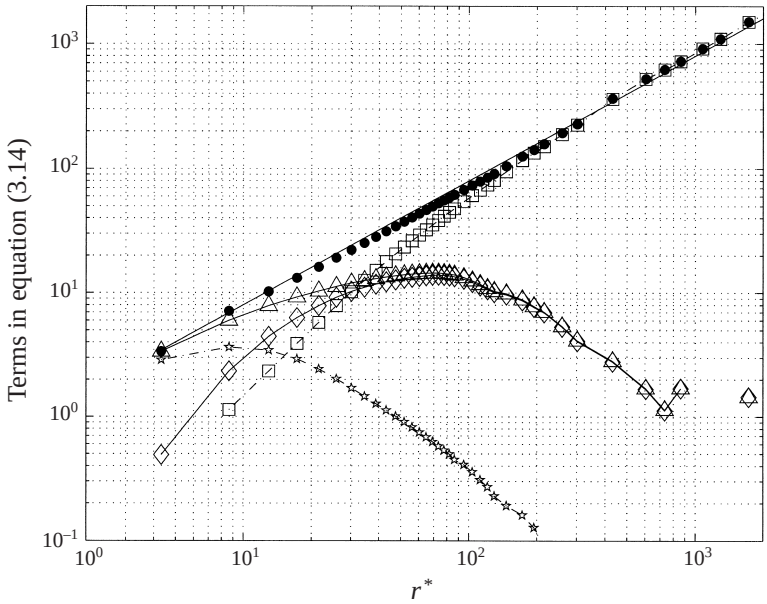

FIGURE 3. Verification of (3.14) at $x_1/M = 70$: $\diamond$, the turbulent transport A (the continuous line is a polynomial interpolation); $\star$, the small-scale diffusion term B (the dotted line is a polynomial interpolation), the straight line is $\frac{4}{5}r^*$; $\square$, the source term S^*_{u1}; $\triangle$, $A + B$; $\bullet$, $A + B + S^*_{u1}$.

required (the 'divergence' advective term $\langle \nabla_{\boldsymbol{x}}(\boldsymbol{u}\theta^2)\rangle$ disappears only because of local homogeneity). Terms which are sensitive to local isotropy (mainly the turbulent transport term A, but also term B), are not present at these large scales. On the contrary, terms which depend on local homogeneity only are present at these large scales.

A generalized form of Kolmogorov's equation (Monin & Yaglom 1975)

$$-\tfrac{4}{5}\langle\epsilon\rangle r = \langle(\Delta u_1)^3\rangle - 6\nu\frac{\mathrm{d}}{\mathrm{d}r}\langle(\Delta u_1)^2\rangle \tag{3.13}$$

can be obtained using a procedure similar to that which led to (3.8). After applying homogeneity and isotropy, all the terms can be written using only Δu_1. Acknowledging that, for grid turbulence, second-order moments of Δu_1 are not stationary, we obtain an additional term:

$$S_{u1} = -3\frac{U_1}{r^4}\int_0^r y^4\frac{\partial}{\partial x_1}\langle(\Delta u_1)^2\rangle \mathrm{d}y.$$

The term S_{u1} is computed in a similar manner to S. The generalization of (3.13) is then written in the same way, in the dimensionless form (using Kolmogorov characteristic variables)

$$\tfrac{4}{5}r^* = A + B + S^*_{u1}. \tag{3.14}$$

Figure 3 reflects the very good agreement we obtain. Note that Kolmogorov's equation is also verified up to 5η only, and that the additional terms in (3.10) and (3.14) are similar, apart from the factors y^2 and y^4, a difference which is just a direct consequence of the different expressions for the operators (3.5) when applied to a scalar and a vector field. The departure from (3.10) at large r (figure 2 and possibly to a smaller

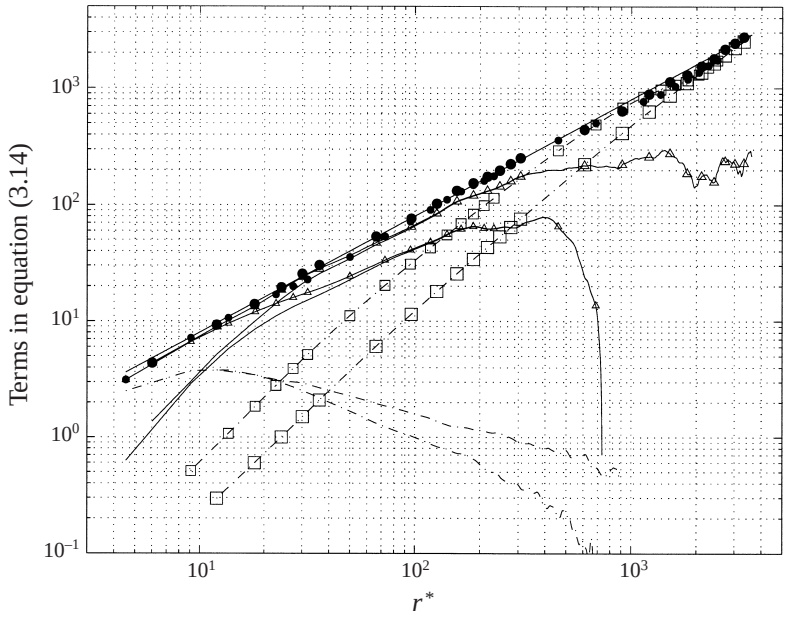

FIGURE 4. Verification of (3.14) for Mydlarski & Warhaft's data. Same symbols as in figure 3. $R_\lambda = 99$: smaller symbols; $R_\lambda = 448$: bigger symbols.

extent figure 3) may reflect a departure from global isotropy. In this context, we have verified that, at large r, $\langle(\Delta u_1)^2\rangle$ and $\langle(\Delta u_2)^2\rangle$ are consistent with the measured anisotropy, namely $\langle u_1^2\rangle/\langle u_2^2\rangle \approx 1.6$.

As emphasized by Frisch (1995, § 6.2.5), in order to derive the four-fifths law (in Kolmogorov's equation), several limits are taken, in this order:

$t \to \infty$ yielding a statistical steady state;

$\nu \to 0$ to eliminate any residual dissipation in the IR;

$r \to 0$ to eliminate the direct influence of the large-scale forcing. Kolmogorov's equation can thus be written, in the IR, using our notation, as

$$\lim_{r\to 0}\lim_{\nu\to 0}\lim_{t\to\infty} \frac{-\langle(\Delta u_1)^3\rangle}{r} = \tfrac{4}{5}\langle\epsilon\rangle. \tag{3.15}$$

The approach proposed herein generalizes (3.15), by eliminating the first limit, $\lim_{r\to 0}$ (which is in fact the last limit in treating the third-order moments). The large-scale influence is therefore taken into account. In the same spirit, we can say that our general approach, i.e. (3.14), could be written as

$$\lim_{\nu\to 0}\lim_{t\to\infty} \frac{-\langle(\Delta u_1)^3\rangle}{r} + \frac{S_{u1}}{r} = \tfrac{4}{5}\langle\epsilon\rangle. \tag{3.16}$$

A final comment pertains to the term 'stationarity' which here has to be understood as the stationarity of all the statistics in a fixed reference frame situated at a certain position x_1/M. Thus, the decay is identified here with a large-scale non-homogeneity, as discussed previously. The same comment applies to Yaglom's equation.

In order to analyse the influence of the Reynolds number R_λ, we have plotted on figure 4 the velocity data obtained by Mydlarski & Warhaft (1996), for $R_\lambda = 99$ and $R_\lambda = 448$, using an active grid. The influence of R_λ on A and B, which are associated

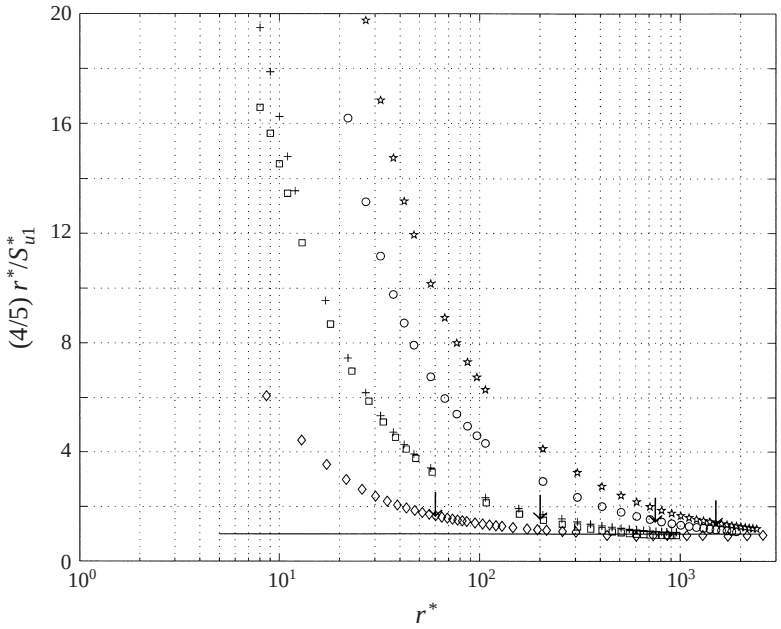

FIGURE 5. Ratio $\frac{4}{5}r^*/S^*_{u1}$ for the present data and those of Mydlarski & Warhaft (1996). Present data: $\diamond$, $R_\lambda = 66$. Mydlarski & Warhaft's data: $\square$, $R_\lambda = 99$; $+$, $R_\lambda = 134$; $\circ$, $R_\lambda = 319$; $\star$, $R_\lambda = 448$. Arrows indicate the value of l^* for each R_λ (except for $R_\lambda = 134$, for which l^* has almost the same value as for $R_\lambda = 99$).

with $-\langle(\Delta u_1)^3\rangle$ and $\langle(\Delta u_1)^2\rangle$, is well known (e.g. Mydlarski & Warhaft 1996; Yeung & Zhou 1997). The new term, S_{u1}, has a markedly stronger influence on IR scales when R_λ is smaller. In particular, for $R_\lambda = 448$, where $-\langle(\Delta u_1^*)^3\rangle$ is very close to $\frac{4}{5}r^*$ for scales as large as about 200η, S_{u1} vanishes rapidly. The quality of agreement between the new relation, (3.14), and all the data sets is essentially independent of R_λ.

Figure 5 expresses more quantitatively the relative importance of S^*_{u1}, in the context of (3.14), with respect to r^* and R_λ. The ratio $\frac{4}{5}r^*/S^*_{u1}$ is shown for the five data sets. For all Reynolds numbers, the new term is about one half of $\frac{4}{5}r^*$ for $r = l$ (l, the integral length scale, was estimated, as in Mydlarski & Warhaft 1996, from $l = 0.9u_1'^3/\langle\epsilon\rangle$). However, larger contributions are obtained for smaller Reynolds numbers, since the maximum level attained by $-\langle(\Delta u_1^*)^3\rangle$ is then significantly smaller than $\frac{4}{5}r^*$ (as already observed in figure 3, for $R_\lambda = 66$).

It is worth pointing out that, for our passive grid, $\langle u_1^2\rangle/\langle u_2^2\rangle \approx 1.60$ whereas, for Mydlarski & Warhaft's 'active grid', this ratio is about 1.45.

Finally, it should be mentioned that the behaviour of the dynamic field, via Kolmogorov's equation, has been extensively examined by Batchelor (1947) and Hill (1997). In both studies, the non-stationarity of the flow was addressed, but no detailed development nor verification were implemented. On the other hand, Frisch (1995) has included a random forcing term, active only at large scales, which is stationary in time and homogeneous in space. The analogy between Yaglom's equation and a more general form of Kolmogorov's equation was pointed out by Antonia *et al.* (1997) and tested in different flows.

4. Conclusion

A generalized form of Yaglom's equation has been proposed for thermal grid turbulence at small Reynolds numbers. The new equation includes an additional source term, related to the non-stationarity of the second-order moments. Equation (3.8) is quite well verified, emphasizing the importance of the non-stationarity in terms of its influence on both the large scales and the inertial range scales. A generalization of Kolmogorov's equation is also proposed and verified with the same degree of accuracy as (3.8). In particular, the present results clearly demonstrate that deviations from the $\frac{4}{3}$ or $\frac{4}{5}$ laws cannot be attributed in a straightforward manner, as is generally done in the literature, to a departure from isotropy. On the contrary, in grid turbulence, we have shown that an additional large-scale contribution evaluated within the isotropy constraints closes Yaglom's and Kolmogorov's equations with quite reasonable accuracy.

Note added in proof: Equation (3.14) was also derived by Saffman (1968) starting from the Kármán–Howarth equation. We became aware of this derivation just before the proof-reading stage and apologize for this omission.

The support of the Australian Research Council is gratefully acknowledged. L. Danaila was supported by a grant from the Ministère des Affaires Etrangères, while visiting the University of Newcastle. We are grateful to L. Mydlarski and Z. Warhaft for their co-operation in making their velocity structure function data available to use. We warmly thank A. Yaglom for the fruitful discussion we had during ETC7. We also thank P. Le Gal for his helpful comments.

REFERENCES

Antonia, R. A., Chambers, A. J. & Browne, L. W. 1983 Relations between structure functions of velocity and temperature in a turbulent jet. *Exps. Fluids* **1**, 213.

Antonia, R. A., Chambers, A. J., Van Atta, C. W., Friehe, C. A. & Helland, K. N. 1978 Skewness of temperature derivative in a heated grid flow. *Phys. Fluids* **21**, 509.

Antonia, R. A., Ould-Rouis, M., Anselmet, F. & Zhu, Y. 1997 Analogy between predictions of Kolmogorov and Yaglom. *J. Fluid Mech.* **332**, 395.

Antonia, R. A., Zhou T. & Zhu, Y. 1998 Three-component vorticity measurements in a turbulent grid flow. *J. Fluid Mech.* **374**, 29.

Batchelor, G. K. 1947 Kolmogoroff's theory of locally isotropic turbulence. *Proc. Camb. Phil. Soc.* **43**, 553.

Boratav, O. N. & Pelz, R. B. 1994 Direct numerical simulations of transition to turbulence from a high-symmetry initial condition. *Phys. Fluids* **6**, 2757.

Budwig, R., Tavoularis, S. & Corrsin, S. 1985 Temperature fluctuations and heat flux in grid-generated isotropic turbulence with streamwise and transverse mean-temperature gradients. *J. Fluid Mech.* **153**, 441.

Comte-Bellot, G. & Corrsin, S. 1966 The use of a contraction to improve the isotropy of grid-generated turbulence. *J. Fluid Mech.* **25**, 657.

Corrsin, S. 1951 On the spectrum of isotropic temperature fluctuations in isotropic turbulence. *J. Appl. Phys.* **22**, 469.

Danaila, L., Zhou, T., Anselmet, F. & Antonia, R. A. 1999 Calibration of a temperature dissipation probe in decaying grid turbulence. *Exps. Fluids* (to appear).

Durbin, P. A. 1982 Analysis of the decay of temperature fluctuations in isotropic turbulence. *Phys. Fluids* **25**, 1328.

Frisch, U. 1995 *Turbulence: The Legacy of A. N. Kolmogorov*. Cambridge University Press.

Hill, R. J. 1997 Applicability of Kolmogorov's and Monin's equations of turbulence. *J. Fluid Mech.* **353**, 67.

Holzer, M. & Siggia, E. D. 1994 Turbulent mixing of a passive scalar. *Phys. Fluids* **6**, 1820.

MESTAYER, P. 1982 Local isotropy and anisotropy in a high-Reynolds-number turbulent boundary layer. *J. Fluid Mech.* **125**, 475.

MONIN, A. S. & YAGLOM, A. M. 1975 *Statistical Fluid Mechanics*, vol. 2. MIT Press.

MYDLARSKI, L. & WARHAFT, Z. 1996 On the onset of high-Reynolds-number grid-generated wind tunnel turbulence. *J. Fluid Mech.* **320**, 331.

MYDLARSKI, L. & WARHAFT, Z. 1998 Passive scalar statistics in high-Péclet-number grid turbulence. *J. Fluid Mech.* **358**, 135.

OBOUKHOV, A. M. 1949 Structure of the temperature field in turbulent flows. *Izv. Akad. Nauk SSSR Geogr. Geofiz.* **13**, 58.

PUMIR, A. 1994*a* A numerical study of the mixing of the passive scalar in three dimensions in the presence of a mean gradient. *Phys. Fluids* **6**, 2118.

PUMIR, A. 1994*b* Small scale properties of scalar and velocity differences in three-dimensional turbulence. *Phys. Fluids* **6**, 3974.

SAFFMAN, P. G. 1968 Lectures on homogeneous turbulence. In *Topics in Nonlinear Physics* (ed. N. Zabusky), pp. 485–614. Springer.

SREENIVASAN, K. R. 1991 On local isotropy of passive scalars in turbulent shear flows. *Proc. R. Soc. Lond.* A **434**, 165.

SREENIVASAN, K. R. 1996 The passive scalar spectrum and the Obukhov-Corrsin constant. *Phys. Fluids* **8**, 189.

SREENIVASAN K. R. & TAVOULARIS, S. 1980 On the skewness of the temperature derivative in turbulent flows. *J. Fluid Mech.* **101**, 783.

SREENIVASAN, K. R., TAVOULARIS, S., HENRY, R. & CORRSIN, S. 1980 Temperature fluctuations and scales in grid-generated turbulence. *J. Fluid Mech.* **100**, 597.

TONG, C. & WARHAFT, Z. 1994 On passive scalar derivative statistics in grid turbulence. *Phys. Fluids* **6**, 2165.

WARHAFT, Z. & LUMLEY, J. L. 1978 An experimental study of the decay of temperature fluctuations in grid-generated turbulence. *J. Fluid Mech.* **88**, 659.

YAGLOM, A. M. 1949 On the local structure of a temperature field in a turbulent flow. *Dokl. Akad. Nauk SSSR* **69**, 743.

YEUNG, P. K. & ZHOU, YE. 1997 Universality of the Kolmogorov constant in numerical simulations of turbulence. *Phys. Rev.* E **56**, 1746.